GROUNDING HIGH DIMENSIONAL REPRESENTATION SIMILARITY BY COMPARING DECODABILITY AND NETWORK PERFORMANCE

Anonymous authors
Paper under double-blind review

ABSTRACT

To understand and interpret neural networks, representation similarity metrics have been used to compare learned representations between and across networks. Recent experiments have compared these similarity metrics to find the best performing and the most robust metrics, noting that classic baselines perform surprisingly well. These experiments are mostly constrained to studying relatively low-dimensional representations because of the computational cost of prominent representation similarity metrics. We extend previous work to test representation similarity metrics on larger convolutional networks processing larger images. In order to make this work possible, we employ reformulated representation similarity metrics for use on very high-dimensional representations. Using these reformulated similarity metrics, we test how well each metric captures changes to representations induced by ablations in two popular convolutional networks. In order to ground the effects of changes to representations in function, we use linear decoding probes and network performance measures. These measures of function allow us to test how well similarity metrics capture changes in decodable information versus changes in network performance. Linear decoding methods index available information in the representation, while network performance measures index the information used by the network. We show that all the tested representation similarity metrics significantly predict changes in network function and decodability. Within these metrics, on average, Procrustes and CKA outperform regularized CCA-based methods. All metrics predict decodability changes significantly better than they do network function. Procrustes and CKA do not outperform regularized CCA-based metrics for all network and functionality measure combinations. We add to the growing literature on representational similarity metrics to facilitate the improvement of current metrics for network interpretability.

1 INTRODUCTION

Neural networks already play a critical role in systems where understanding and interpretation are paramount like in self-driving cars and judicial courts. To understand and interpret neural networks, representation similarity metrics have been used to compare learned representations between and across networks (Kornblith et al. (2019); Raghu et al. (2017); Morcos et al. (2018b); Wang et al. (2018); Li et al. (2015); Feng et al. (2020)). Using these similarity metrics, researchers evaluate whether networks trained from different random initializations learn the same information, whether different layers learn redundant or complementary information, and how different datasets affect learning (Kornblith et al. (2019); Li et al. (2015); Wang et al. (2018)). Apart from helping to answer these fundamental questions, similarity metrics have the potential to provide a useful tool for quantifying the differences between high-dimensional representation spaces.

What it means for representations to be similar is not straightforward. Many similarity metrics have been proposed with different underlying assumptions and strategies for comparing representation spaces. These different assumptions and strategies can lead to quantitatively different predictions. For instance, Ding et al. (2021) statistically test similarity metrics to determine their sensitivities to important changes in representations. Namely, they test to see if similarity metrics can discriminate between representations with different functional properties. To vary these properties, they perturb

representations in pre-trained networks and measure how those perturbations change linear probe decoding accuracies and the network's performance on out-of-distribution tasks. They show that these induced functional changes do not always correlate well with metric similarities between the intact and perturbed representations. Some metrics capture some of the functional changes and pass some of the statistical tests, but no one metric passes all of them. It is therefore unclear which representation similarity metrics capture the functional properties of representations and further tests are needed to evaluate them.

In addition to extensive evaluation in established areas, expanding the scope of evaluations to new and larger problems provides a more general understanding of the relationship between similarity metrics and network function. Unfortunately, a computational barrier prohibits the field from testing certain representation similarity metrics on larger networks. The computational barrier arises because prominent representation similarity metrics frequently require computing a feature covariance matrix between the two compared representation matrices. The computational cost of generating and storing this matrix grows prohibitively large as the number of neurons in each representation grows. As a result, previous works examining certain representation similarity metrics have focused on studying relatively small representations with less than 1000 neurons. We drastically reduce the computational cost by reformulating prominent representation similarity metrics (CKA, Procrustes, and some CCA-based methods) to avoid the cost of directly computing the full covariance matrix (as others have done for other metrics, i.e. SVCCA Raghu et al. (2017)). Using these reformulations, we extend previous work to test representation similarity metrics on larger convolutional networks processing larger images.

Inspired by the procedure outlined by Ding et al. (2021), we systematically test how well each representation similarity metric captures changes to representations induced by ablations in the relatively larger AlexNet and MobileNetV2 networks. We quantify the changes induced by altering representations by observing the changes in functional measures of the representation's behavior. We utilize linear probes and network performance, focusing on the same downstream image categorization task. These functional measures allow us to test how well representation similarity metrics capture changes in decodable information versus changes in network performance. Linear probes measure how much task-specific information is directly decodable from a given representation. On the other hand, network performance measures quantify the usefulness of a given representation for the network trained on the task. By directly comparing linear probe accuracies and network performances on the same task we can answer questions like: how much more sensitive are representation similarity metrics to linear properties of the representation compared to the downstream non-linear properties utilized by the network? Answering these questions may help in the development of interpretability methods that are increasingly sensitive to actual network function.

In this work, we show that CKA, Procrustes, and regularized CCA-based representation similarity metrics significantly predict changes in network function and decodability. Within these metrics, on average, Procrustes and CKA outperform regularized CCA-based methods. All the tested metrics predict decodability changes significantly better than they do network function. Procrustes and CKA do not outperform regularized CCA-based metrics on all network and functionality measure combinations. In general, this paper documents the following contributions:

- To facilitate the use of representation similarity metrics on high-dimensional representation matrices, we reformulate CKA, Procrustes, and CCA-based metrics to drastically reduce their computational cost. These reformulations allow us to apply the reformulated metrics to CNNs trained on ImageNet.
- We extend the work of Ding et al. (2021) to show that five prominent representation similarity metrics are significantly sensitive to functional measures of image classification in two popular convolutional neural networks.
- We also compare linear decoding and network performance functional measures, finding that the changes in tested metrics are associated with changes in linear probing accuracies and network performance deficits. In this comparison we also show that all five metrics are more strongly associated with linearly decodable information.
- Within the tested metrics, we show that Procrustes and CKA tend to outperform regularized CCA-based methods, but that tests using linear probes and network performance based functional measures can produce different results in different networks.

- Across all our experiments, we rigorously apply hierarchical linear models to test the effects of metric and functionality choices.

2 METHODS

In Section 2.1, we describe the statistical testing methodology used in our experiments. In Section 2.2, we introduce the representation similarity measures we evaluate and reformulate them for use on very high-dimensional representations. In Section 2.3, we describe how we use ablation to produce representations with different functional properties. Finally, in Section 2.4, we describe how we use linear probe decoding deficits and class-specific performance deficits to measure decodable and downstream network changes, respectively, in the ablated representations.

2.1 STATISTICAL TESTING

Assume $\boldsymbol{A} \in \mathbb{R}^{n \times p_1}$ represents a matrix of activations for p_1 neurons given n examples, and $\boldsymbol{B} \in \mathbb{R}^{n \times p_2}$ represents a matrix of activations for p_2 neurons given the same n examples. The matrices $\boldsymbol{A}$ and $\boldsymbol{B}$ are called representation matrices and have been preprocessed to have centered columns. Let $d(\boldsymbol{A}, \boldsymbol{B})$ denote a representation similarity metric that returns zero if and only if $\boldsymbol{A} = \boldsymbol{B}$ and for which $d(\boldsymbol{A}, \boldsymbol{B}) = d(\boldsymbol{B}, \boldsymbol{A})$. These metrics do not satisfy the triangle inequality and are therefore not formal distance metrics. For simplicity, we will refer to them as metrics in this work.

To quantify functional differences between representation matrices, we use functional behavior measures. Formally, let $f : \mathbb{R}^{n \times p} \to \mathbb{R}$ denote a functional behavior measure that, given a representation matrix, returns a scalar measure of the representation's role in function. In this study, we utilize two functionality measures, class-specific linear decoding accuracy (f_{decoding}) and class-specific network performance ($f_{\text{performance}}$). In the case of linear decoding accuracy, f_{decoding} returns the average linear probe accuracy achieved from decoding a target class identity from a representation matrix. On the other hand, $f_{\text{performance}}$ returns the average classification performance for a target class achieved by feeding the representation matrix to the network at the appropriate layer. More details are presented in Section 2.4.

As in Ding et al. (2021), we aim to statistically test representation similarity metrics using the same methodology according to their paper:

1. Gather S, a set of representation matrices that vary along one or more dimensions. We note that S contains unablated as well as ablated representation matrices (see Section 2.3).
2. Select an unablated reference matrix $\boldsymbol{X} \in S$.
3. Compute the following for all $\boldsymbol{A}_i \in S$ where $\boldsymbol{A}_i \neq \boldsymbol{X}$:
   - D $= d(\boldsymbol{X}, \boldsymbol{A}_i)$
   - F $= |f(\boldsymbol{X}) - f(\boldsymbol{A})|$
4. Compute the correlation between D and F using Spearman's correlation.

This procedure quantifies the extent to which the representation similarity metrics, $d(\cdot)$, capture the functionality differences, as measured by $f(\cdot)$, produced by ablating the representation matrix.

2.2 REPRESENTATION SIMILARITY METRICS

As in Ding et al. (2021), we study three main representation similarity metrics: centered kernel alignment (CKA), Procrustes, and projection-weighted canonical correlation analysis (PWCCA).

Centered kernel alignment (CKA) is based on the idea that similar representations also have similar relations between examples. In other words, representation matrices that store images of lettuce and rabbits using similar vectors should be more similar to each other than with representation matrices that encode images of lettuce and dinner plates using similar vectors. This idea leads Kornblith et al. (2019) to formulate linear CKA, which uses a linear kernel to compare example vectors (henceforth referred to as just CKA):

$$d_{\text{CKA}}(\boldsymbol{A}, \boldsymbol{B}) = 1 - \frac{\|\boldsymbol{A}^{\text{T}}\boldsymbol{B}\|_{\text{F}}^2}{\|\boldsymbol{A}^{\text{T}}\boldsymbol{A}\|_{\text{F}}\|\boldsymbol{B}^{\text{T}}\boldsymbol{B}\|_{\text{F}}} \tag{1}$$

where $\|\cdot\|_{\mathrm{F}}$ is the Frobenius norm and $\|\boldsymbol{A}^{\mathrm{T}}\boldsymbol{B}\|_{\mathrm{F}}^2$ derives from the following relation:

$$\langle \mathrm{vec}(\boldsymbol{A}\boldsymbol{A}^{\mathrm{T}}), \mathrm{vec}(\boldsymbol{B}\boldsymbol{B}^{\mathrm{T}})\rangle = \mathrm{tr}(\boldsymbol{A}\boldsymbol{A}^{\mathrm{T}}\boldsymbol{B}\boldsymbol{B}^{\mathrm{T}}) = \|\boldsymbol{A}^{\mathrm{T}}\boldsymbol{B}\|_{\mathrm{F}}^2 \tag{2}$$

Relation 2 shows that the similarity between pairwise example similarity matrices (far left) is equal to the squared Frobenius norm of the feature covariance matrix between representations (far right). Kornblith et al. (2019) use this relation to form Equation 1 which measures the normalized similarity between the example similarity matrices of $\boldsymbol{A}$ and $\boldsymbol{B}$. Unfortunately, computing and storing either $\boldsymbol{A}^{\mathrm{T}}\boldsymbol{B}$, $\boldsymbol{A}^{\mathrm{T}}\boldsymbol{A}$, or $\boldsymbol{B}^{\mathrm{T}}\boldsymbol{B}$ can be prohibitively expensive when both p_1 and p_2 grow too large. Therefore we reformulate Equation 1 using relation 2 and the fact that $\|\boldsymbol{X}^{\mathrm{T}}\boldsymbol{X}\|_{\mathrm{F}} = \|\boldsymbol{X}\boldsymbol{X}^{\mathrm{T}}\|_{\mathrm{F}}$ into:

$$d_{\mathrm{CKA}}(\boldsymbol{A}, \boldsymbol{B}) = 1 - \frac{trace(\boldsymbol{A}\boldsymbol{A}^{\mathrm{T}}\boldsymbol{B}\boldsymbol{B}^{\mathrm{T}})}{\|\boldsymbol{A}\boldsymbol{A}^{\mathrm{T}}\|_{\mathrm{F}}\|\boldsymbol{B}\boldsymbol{B}^{\mathrm{T}}\|_{\mathrm{F}}} \tag{3}$$

This reformulation allows us to use CKA on layers with at least 100 times more neurons than previous studies.

Procrustes is an analytical solution to the orthogonal Procrustes problem which involves finding a right rotation of matrix $\boldsymbol{B}$ that is as close as possible to $\boldsymbol{A}$ as measured by the Frobenius norm:

$$d_{\mathrm{Procrustes}}(\boldsymbol{A}, \boldsymbol{B}) = \|\boldsymbol{A}\|_{\mathrm{F}}^2 + \|\boldsymbol{B}\|_{\mathrm{F}}^2 - 2\|\boldsymbol{A}^{\mathrm{T}}\boldsymbol{B}\|_* \tag{4}$$

where $\|\cdot\|_*$ is the nuclear norm. As with CKA, $\boldsymbol{A}^{\mathrm{T}}\boldsymbol{B}$ needs to be replaced to lighten the computational cost of working with large layers. Therefore, we utilize the fact that the nuclear norm of a matrix is the sum of its singular values to reformulate Procrustes:

$$d_{\mathrm{Procrustes}}(\boldsymbol{A}, \boldsymbol{B}) = \|A\|_{\mathrm{F}}^2 + \|B\|_{\mathrm{F}}^2 - 2\sum_{i}^{n} \sqrt{\lambda_i(\boldsymbol{A}\boldsymbol{A}^{\mathrm{T}}\boldsymbol{B}\boldsymbol{B}^{\mathrm{T}})} \tag{5}$$

where $\lambda_i(\boldsymbol{X})$ represents the ith eigenvalue of matrix $\boldsymbol{X}$. Again, this reformulation saves us from manipulating the large $p_1 \times p_2$ matrix by replacing it with a much smaller $n \times n$ matrix (assuming $n \ll p_1, p_2$).

Projection-weighted canonical correlation analysis (PWCCA) is a special case of canonical correlation analysis (CCA) proposed by Morcos et al. (2018a). CCA itself provides a solution to the problem of linearly projecting $\boldsymbol{A}$ and $\boldsymbol{B}$ into a shared subspace where their correlations are maximized. CCA finds $\min(p_1, p_2)$ pairs of weight vectors ($\boldsymbol{w_A}$,$\boldsymbol{w_B}$) and the resulting correlation induced by projecting $\boldsymbol{A}$ and $\boldsymbol{B}$ using the ith weight vector is:

$$\begin{aligned} \rho_i = \max_{\boldsymbol{w}_{\boldsymbol{A}}^i, \boldsymbol{w}_{\boldsymbol{B}}^i} \ & \mathrm{corr}(\boldsymbol{A}\boldsymbol{w}_{\boldsymbol{A}}^i, \boldsymbol{B}\boldsymbol{w}_{\boldsymbol{B}}^i) \\ \text{subject to} \quad \forall_{j<i} \quad & \boldsymbol{A}\boldsymbol{w}_{\boldsymbol{A}}^i \perp \boldsymbol{A}\boldsymbol{w}_{\boldsymbol{A}}^j \\ & \boldsymbol{B}\boldsymbol{w}_{\boldsymbol{B}}^i \perp \boldsymbol{B}\boldsymbol{w}_{\boldsymbol{B}}^j \end{aligned} \tag{6}$$

where the ρ_i is maximized subject to the constraint that the subspace features be orthogonal. Equation 6 can be solved for by performing singular value decomposition on $(\boldsymbol{A}^{\mathrm{T}}\boldsymbol{A})^{-1/2}\boldsymbol{A}^{\mathrm{T}}\boldsymbol{B}(\boldsymbol{B}^{\mathrm{T}}\boldsymbol{B})^{-1/2}$ where the singular values are equal to the correlations ($\rho_i \ \forall \ i \in [1, ..., \min(p_1, p_2)]$).

However, the inverses of the feature covariance matrices do not exist when the number of neurons exceeds the number of examples. For these cases, we can use regularized or "ridge" CCA (Vinod (1976)), which applies an L_2 penalty to the weight vectors and can be solved by performing SVD on $(\boldsymbol{A}^{\mathrm{T}}\boldsymbol{A} + \kappa_{\boldsymbol{A}}\boldsymbol{I})^{-1/2}\boldsymbol{A}^{\mathrm{T}}\boldsymbol{B}(\boldsymbol{B}^{\mathrm{T}}\boldsymbol{B} + \kappa_{\boldsymbol{B}}\boldsymbol{I})^{-1/2}$. However, we again run into the problem that the feature covariance matrices are too costly to compute for large layers. So, we employ the "kernel trick" introduced by Kuss & Graepel (2003) and Hardoon et al. (2004) and refined by Tuzhilina et al. (2021) which allows us to substitute into the above expression $\boldsymbol{R_A}$ for $\boldsymbol{A}$ where $\boldsymbol{R_A}$ represents an $n \times n$ matrix recovered by applying SVD on $\boldsymbol{A}$, i.e. $\boldsymbol{A} = \boldsymbol{R_A}\boldsymbol{V_A}^{\mathrm{T}}$. The same trick can be applied to $\boldsymbol{B}$. These substitutions allows us to work with much smaller matrices and make CCA computationally tractable for large layers. The only drawback is that if we apply the "kernel trick" to both matrices, we recover only n canonical correlations rather than $\min(p_1, p_2)$.

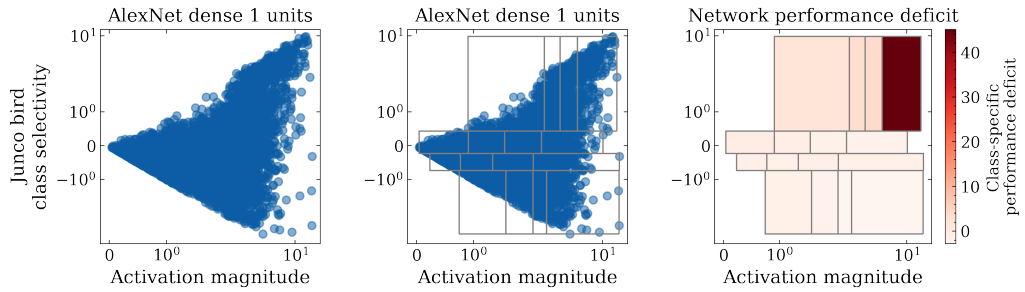

(a) (b) (c)

Figure 1: **Grouping of units for ablation by class selectivity and activation magnitude.** a). An example of the reduced activation space for the junco bird class and AlexNet. The vertical axis measures a unit's average selectivity for the junco bird class. The horizontal axis measures a unit's average magnitude of activation. Each point represents a unit in the Dense 1 layer. b). We constructed a grid to overlay on the activation space so that each cell of the grid contained the same number of units. c). After overlaying the grid, we ablated each group of units and measured causal class-specific performance deficits.

Mean CCA (as used by Raghu et al. (2017)) and mean squared CCA (Ramsay et al. (1984)) average raw and squared correlations recovered through CCA, respectively. However, PWCCA re-weights each correlation value by its importance for the underlying representation. Formally, if representation matrix $\boldsymbol{A}$ has neuron activation vectors $[\boldsymbol{z}_1, ..., \boldsymbol{z}_{p_1}]$ and CCA vectors $[\boldsymbol{h}_1, ..., \boldsymbol{h}_n]$, then PWCCA computes a weighted mean as:

$$d_{\text{PWCCA}}(\boldsymbol{A}, \boldsymbol{B}) = 1 - \sum_{i=1}^{n} \tilde{\alpha}_i \rho_i \quad \text{s.t.} \quad \alpha_i = \sum_j |\langle \boldsymbol{h}_i, \boldsymbol{z}_j \rangle|$$

where $\tilde{\alpha}_i$ is a normalized version of α_i. The preceding CCA reformulations represent regularized forms of CCA-based metrics useful for high-dimensional representations, which we refer to as regularized CCA-based metrics in the text, but just CCA metrics in the figures for sake of brevity.

2.3 Ablation

To study network functionality changes, we needed to develop a method for manipulating representations to reliably produce network performance deficits at the output of the network. We found that selectively deleting neurons from a CNN layer with similar average activation profiles reliably produced class-specific classification deficits at the output of the CNN. Specifically, for each of the 10 target classes and layer of the CNNs we tested, AlexNet and MobileNetV2, we first projected every neuron onto two dimensions: class selectivity and activation magnitude (Figure 1a). Then, we constructed a grid to overlay on the activation space so that each cell of the grid contained the same number of neurons (Figure 1b). To supply the set S of representation matrices from Section 2.1, we ablated one cell of neurons at a time by setting the activation values for those neurons to zero. Figure 1c shows the class-specific performance deficit (detailed in the next section) for the junco bird class caused by ablating each cell of units in the grid.

2.4 Functionality measures

After collecting the set S of ablated representation matrices, we sought to compare two functionality measures. First, as in Ding et al. (2021), we fit linear probe decoders to each representation matrix in S. With the linear probes we aimed to decode the identity of one target class, so we fit simple logistic regression classifiers to distinguish the target class representations from all other representations in the representation matrix. Because many of the CNN layers contained thousands of features, we randomly selected 100 neurons as features in the logistic regression model and averaged the training accuracy over 200 repetitions as in Alain & Bengio (2016). Intuitively, the accuracies measure how much information a representation matrix contains about the target class. We refer to the changes induced in the decodability of the target class by ablation as decoding accuracy deficits.

In contrast to linear decoding accuracies, we also measured the network's class-specific classification performance when utilizing the representations in the representation matrix during inference. Specifically, we recorded the average classification rank of the target class. For instance, if the CNN's softmax layer predicted that the Junco bird class was the third most likely class given an image of a Junco bird, then that image received a rank of three. The average class-specific ranks intuitively measure how functionally useful the representations from the representation matrix were to the network. We refer to the changes induced in class-specific classification rank by ablation as network performance deficits.

3 RESULTS

In this section, we detail the results of aggregating our statistical tests across each layer and class from AlexNet and MobileNetV2. We conducted a hierarchical linear model to evaluate the prediction of the rank correlation values as a function of two factors: 1) *metric*, i.e. CKA, Procrustes, and regularized CCA-based methods and 2) *functionality*, i.e. network performance deficits and decoding accuracy deficits. To allow for comparable correlation coefficients, we fisher-z transformed each rank correlation value, then, averaged them across layers for each each metric and functionality. Afterwards, we inverse transformed the fisher-z back to correlation coefficients. We modeled classes as random units. To sum, the transformed correlation values were modeled as a function of metric type and functionality measure. All analyses were conducted using the "lme4" package in R (Bates et al. (2014)). Figures were generated using "ggplot2" (Wickham (2016), "raincloudplots" (Allen et al. (2021)), and "smplot" package (Min & Zhou (2021)) in R.

3.1 CORRELATION VALUES ARE SIGNIFICANTLY ASSOCIATED WITH ABLATION CHANGES IN THE REPRESENTATION

Figure 2a shows the distribution of correlation values across functionality measures. In both cases, the rank correlation values of both functionality measures are significantly different from 0, suggesting that the correlation values are sensitive to functional behavioral changes in the representations, ($F(1,9) = 128.07$, $p < .001$ for AlexNet, $F(1,9) = 1464.06$, $p < .001$ for MobileNetV2). In addition, these correlation values are significantly different between network performance deficits and decoding accuracy deficits, when averaging across the five similarity metrics — CKA, Procrustes, and regularized CCA-based metrics ($F(1,81) = 423.07$, $p < .001$). In other words, there is a significant main effect of functionality. Likewise, Figure 2b shows the same results for MobileNetV2 ($F(1,81) = 5770.037$, $p < .001$).

3.2 CKA AND PROCRUSTES TEND TO OUTPERFORM OTHER METRICS

Figures 3a and 3b show that CKA and Procrustes have, on average, higher rank correlation values compared to the other CCA-based metrics ($t(81) = 4.501$, $p < .0001$ for AlexNet; $t(81) = 15.70$, $p < .0001$ for MobileNetV2). Again, higher rank correlation values indicate a higher coupling between functionality measures and representation similarity metrics, thereby suggesting that CKA and Procrustes are better metrics at capturing functionality.

3.3 FUNCTIONALITIES PRODUCE DIFFERENT RESULTS FOR DIFFERENT NETWORKS

Figure 4 (top) shows a significant interaction between functionality measures and similarity metrics for AlexNet ($F(4,81) = 3.92$, $p < .01$). Figure 4 (bottom) shows the same model for MobileNetV2, however, interaction is non-significant ($F(4,81) = .878$, *N.S.*) In the case of AlexNet, with the plotted means, it is evident that the interaction is driven by the metric differences within decoding accuracy deficits. As for the similarity metrics within network performance deficits, no single metric outperforms the other; instead, each metric achieves a similarly low correlation amongst the network performance deficit group. As for the decoding accuracy deficit group, on the other hand, CKA and Procrustes outperform the CCA-based metrics ($t(81) = 5.697$, $p < .0001$). In the case of MobileNetV2, there is no significant interaction. CKA and Procrustes outperform the CCA-based metrics on both decoding ($t(81) = 12.414$, $p < .0001$) and network performance tests ($t(81) = 9.79$, $p < .0001$), thereby canceling out an interaction effect.

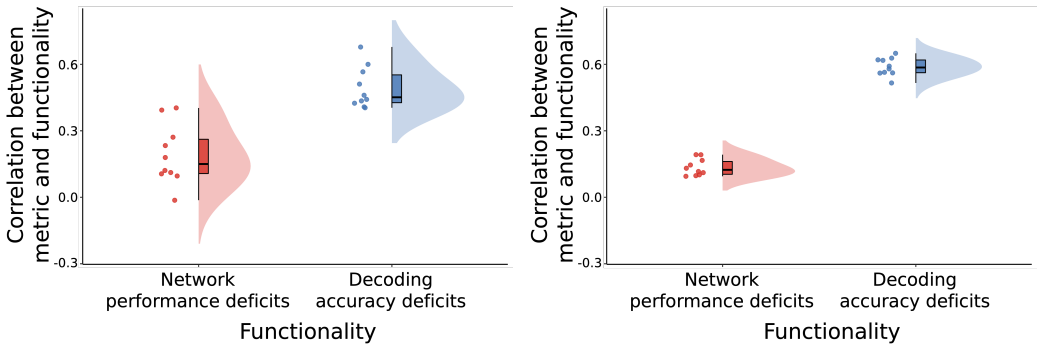

(a) AlexNet (b) MobileNetV2

Figure 2: **Correlation values overall are significantly sensitive to ablation changes in the representations, however, decoding accuracy has a higher value than network performance deficits.** This figure shows the distribution of rank correlation values between functionality measures, i.e., the main effect of functionality measure on AlexNet (a) and MobileNetV2 (b). Each data point represents a value from the ten classes; within each class, we average the five metrics of CKA, Procrustes, PWCCA, mean CCA and mean squared CCA. The distribution is further depicted by the violin plots and boxplots, which illustrates the median and upper/lower quartile of the distribution. Overall, both functionality measures are significantly different from 0, indicating that the rank correlation values are sensitive to changes produced by ablations in the representations. Further examining the difference between functionality measures, we see that the rank correlation values of decoding accuracy deficit are higher than that of network performance deficits. Note that all CCA-based metrics are regularized in our formulations.

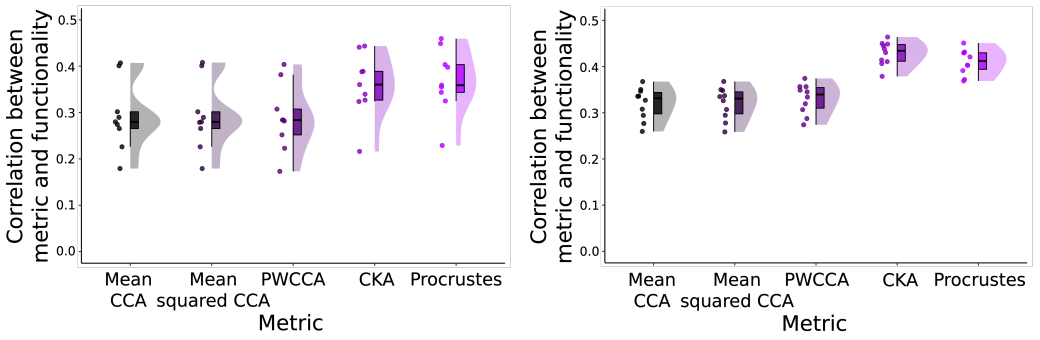

(a) AlexNet (b) MobileNetV2

Figure 3: **CKA and Procrustes outperform CCA-based metrics.** This figure shows the distribution of rank correlation values across each metric, averaged between functionality measures on AlexNet (a) and MobileNetV2 (b). Within each distribution, each data point represents the average rank correlation value from the ten classes, collapsed across network performance deficits and decoding accuracy deficits. Higher rank correlation values in the CKA and Procrustes condition indicate that these metrics are sensitive to the perturbations in the representations compared to other CCA-based metrics. Note that all CCA-based metrics are regularized in our formulations.

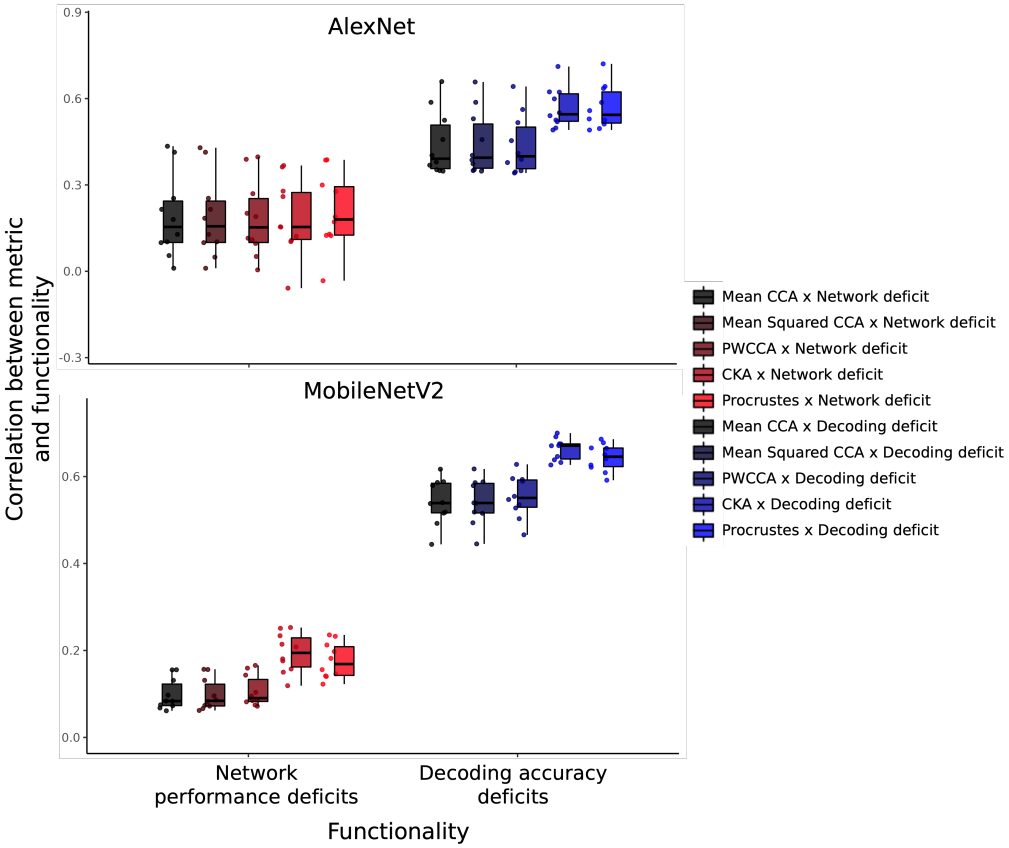

Figure 4: **Pattern of similarity metrics differs depending on functionality measure.** This figure shows a significant interaction between functionality and metric for Alexnet (top) and a non-significant interaction for MobileNetV2 (bottom). In the case of AlexNet, each of the five metrics behave differently depending on functionality type: the five similarity metrics within the network performance deficits condition are not significantly different, whereas metrics do differ within the decoding accuracy deficits condition. Specifically, the CKA and Procrustes metric is significantly different from the CCA-based metrics, only in the decoding accuracy deficit condition. In contrast, in the case of MobileNetV2, this interaction is no longer prominent: CKA and Procrustes consistently outperform CCA-based measures on both functionality tests in MobileNetV2. Note that all CCA-based metrics are regularized in our formulations.

4 DISCUSSION

In this work, we systematically test representation similarity metrics on ImageNet-trained CNNs to determine how sensitive they are to network performance and decoding changes in representations. To facilitate these tests, we reformulate previously proposed similarity metrics to make them computationally tractable for use on high-dimensional representations. Our tests revealed that, while similarity metrics significantly associate with network performance and decoding measures of functionality, they are significantly less sensitive to network performance. Additionally, in most of our tests CKA and Procrustes significantly outperform CCA-based methods. However, we do find that different networks and different functionality choices can eliminate their advantages.

Overall, the results of our experiments are encouraging. All of the representation similarity metrics we tested seem to work well on representations in the large convolutional networks we tested. However, some metrics perform better than others. Ding et al. (2021) previously showed that Procrustes tends to outperform CKA and CCA-based methods on language models. In our experiments on larger image classification models, both CKA and Procrustes tend to perform better than regularized CCA-based methods adapted for larger representations. These results are hinted at by Ding et al. (2021) who show that CKA and Procrustes perform well on image decoding tests, but omit comparisons to CCA-based metrics. Interestingly, CKA and Procrustes did not outperform other methods in all of our experiments. For AlexNet, network performance tests show that all the similarity metrics equally capture network function (Figure 4). This discrepancy may suggest that the best representation similarity metric can change according to the network tested and the functionality used.

In the very least, representation similarity metrics excel to different degrees depending on the choice of functionality. Specifically, all the metrics studied are significantly more sensitive to linear probing functionalities compared to functionalities based on network performance. This finding reflects the considerations made in developing these similarity metrics. Representation similarity metrics were designed to compare the linear geometric properties of two representation spaces. So, it is not surprising that similarity metrics correlate with changes in decoding accuracies. On the other hand, network performance measures of function reflect how the network utilizes representations. In this case, functionally similar representations are those representations that remain similar after a series of non-linear transformations through layers of the network. Perhaps it is not surprising that this non-linear notion of similarity is harder to capture using current similarity metrics. However, it is the ultimate goal of interpretability to link representation and non-linear network function.

5 LIMITATIONS

We acknowledge the following limitation in this work. Reformulating CCA-based measures to accommodate representations with more neurons than examples required using a regularized version of CCA called "ridge" CCA. In utilizing "ridge" CCA we had to choose regularization penalties to apply to each representation matrix. These penalties were chosen to be consistent across all tests, but were not cross-validated. Future works would benefit from testing more penalty settings to explore their effect on similarity results.

6 CONCLUSION

Taken altogether, the results of this study suggest that representation similarity metrics may already serve well as tools for comparing the geometries of representational spaces, but could be enhanced in order to capture non-linear network function. To illustrate this point, we offer the following thought experiment. Shuffling the indices of a representation has no affect on decoding performance. Similarly, the studied similarity metrics predict no differences between representations and the same representations with shuffled indices. However, a network's performance changes dramatically when its representation indices are shuffled. This thought experiment suggests that understanding the functional role of representation requires looking beyond its inherent geometry to its connections with other parts of the network. Therefore we think it's extremely important to include network performance as a functional measure of representation in future interpretability studies.

7 REPRODUCIBILITY STATEMENT

To ensure the reproducibility of the current work, we have included the code used to conduct and run each of the experiments with the submission. In addition to the code, we have also included in the submission the raw data collected during each of our conducted experiments. At the request of reviewers or other interested parties, additional data sources (i.e. the exact image set used, the representation matrices, etc.) can be made available.

REFERENCES

Guillaume Alain and Yoshua Bengio. Understanding intermediate layers using linear classifier probes. *arXiv preprint arXiv:1610.01644*, 2016.

Micah Allen, Davide Poggiali, Kirstie Whitaker, Tom Rhys Marshall, Jordy van Langen, and Rogier A. Kievit. Raincloud plots: a multi-platform tool for robust data visualization. *Wellcome Open Research*, 4(63), 2021.

Douglas Bates, Martin Mächler, Ben Bolker, and Steve Walker. Fitting linear mixed-effects models using lme4. *arXiv preprint arXiv:1406.5823*, 2014.

Frances Ding, Jean-Stanislas Denain, and Jacob Steinhardt. Grounding representation similarity with statistical testing. *arXiv preprint arXiv:2108.01661*, 2021.

Yunzhen Feng, Runtian Zhai, Di He, Liwei Wang, and Bin Dong. Transferred discrepancy: Quantifying the difference between representations. *arXiv preprint arXiv:2007.12446*, 2020.

David R Hardoon, Sandor Szedmak, and John Shawe-Taylor. Canonical correlation analysis: An overview with application to learning methods. *Neural computation*, 16(12):2639–2664, 2004.

Simon Kornblith, Mohammad Norouzi, Honglak Lee, and Geoffrey Hinton. Similarity of neural network representations revisited. In *International Conference on Machine Learning*, pp. 3519–3529. PMLR, 2019.

Malte Kuss and Thore Graepel. The geometry of kernel canonical correlation analysis. 2003.

Yixuan Li, Jason Yosinski, Jeff Clune, Hod Lipson, and John Hopcroft. Convergent learning: Do different neural networks learn the same representations? *arXiv preprint arXiv:1511.07543*, 2015.

Seung Hyun Min and Jiawei Zhou. smplot: An r package for easy and elegant data visualization. *Frontiers in Genetics*, 12, 2021. doi: 10.3389/fgene.2021.802894.

Ari Morcos, Maithra Raghu, and Samy Bengio. Insights on representational similarity in neural networks with canonical correlation. *Advances in Neural Information Processing Systems*, 31, 2018a.

Ari S Morcos, David GT Barrett, Neil C Rabinowitz, and Matthew Botvinick. On the importance of single directions for generalization. *arXiv preprint arXiv:1803.06959*, 2018b.

Maithra Raghu, Justin Gilmer, Jason Yosinski, and Jascha Sohl-Dickstein. Svcca: Singular vector canonical correlation analysis for deep learning dynamics and interpretability. *Advances in neural information processing systems*, 30, 2017.

JO Ramsay, Jos ten Berge, and GPH Styan. Matrix correlation. *Psychometrika*, 49(3):403–423, 1984.

Elena Tuzhilina, Leonardo Tozzi, and Trevor Hastie. Canonical correlation analysis in high dimensions with structured regularization. *Statistical Modelling*, pp. 1471082X211041033, 2021.

Hrishikesh D Vinod. Canonical ridge and econometrics of joint production. *Journal of econometrics*, 4(2):147–166, 1976.

Liwei Wang, Lunjia Hu, Jiayuan Gu, Zhiqiang Hu, Yue Wu, Kun He, and John Hopcroft. Towards understanding learning representations: To what extent do different neural networks learn the same representation. *Advances in neural information processing systems*, 31, 2018.

Hadley Wickham. *ggplot2: Elegant Graphics for Data Analysis*. Springer-Verlag New York, 2016. ISBN 978-3-319-24277-4. URL https://ggplot2.tidyverse.org.

A APPENDIX

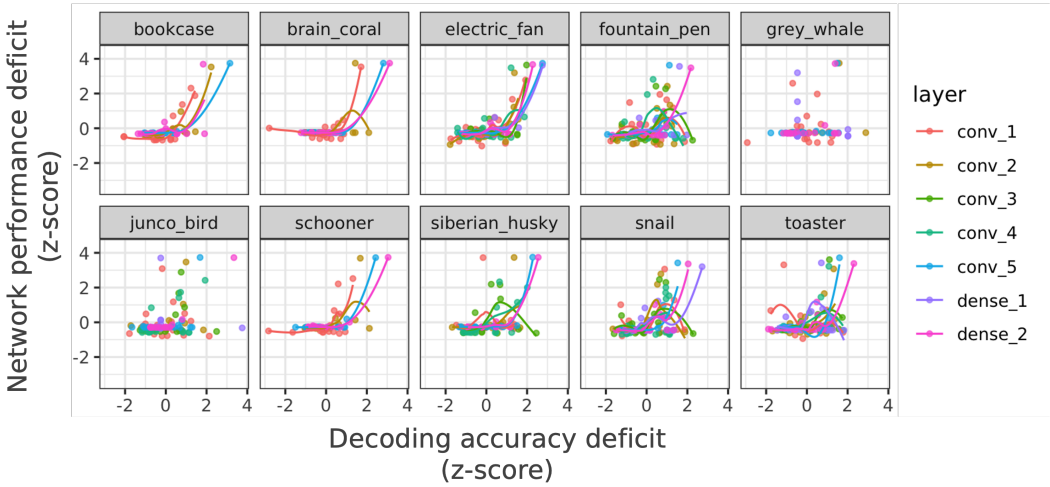

Figure 5: **Decoding accuracy and network performance deficits correlate in later layers of AlexNet.** This figure shows the the relationship between network performance deficit and decoding accuracy deficit across layers and classes in AlexNet, using Local Polynomial Regression Fitting. In later layers of the network, ablations that produce high decoding accuracy deficits also tend to produce high network performance deficits (as illustrated by the fitted lines in the later layers). This relationship does not typically hold for early layers. Note that some points are missing in the case where ablations for certain layer and class combinations did not produce decoding deficits.